Histol Histopathol (2013) 28: 1473-1481
DOI: 10.14670/HH-28.1473

http://www.hh.um.es

Histology and Histopathology
Cellular and Molecular Biology

The vertebrae of prematurely aging mice as a skeletal model of involutional osteoporosis

Sergio Portal-Núñez[1], Julia Cruces[2], Irene Gutiérrez-Rojas[3], Daniel Lozano[1], Juan Antonio Ardura[1], María L. Villanueva-Peñacarrillo[3], Mónica De la Fuente[2] and Pedro Esbrit[1]

[1]Laboratorio de Metabolismo Mineral y Óseo, Instituto de Investigación Sanitaria (IIS)-Fundación Jiménez Díaz; Red Temática de Investigación Cooperativa en Envejecimiento y Fragilidad (RETICEF), Instituto de Salud Carlos III (ISCIII), Madrid, Spain, [2]Departamento de Fisiología Animal (Fisiología Animal II), Universidad Complutense de Madrid (UCM); RETICEF, ISCIII, Madrid, Spain and [3]Departamento de Metabolismo, Nutrición y Hormonas, IIS-Fundación Jiménez Díaz; Centro de Investigaciones Biomédicas en Red de Diabetes y Enfermedades Metabólicas Asociadas (CIBERDEM), ISCIII, Madrid, Spain

Summary. Oxidative stress in bone increases with age, which leads to bone frailty and a high fracture risk. Animal models show that early changes in trabecular structure occur in age-related osteopenia. These models might be valuable to assess the contribution of oxidative stress in age-related bone loss. Premature aging mice (PAM) have previously been characterized as a model of premature immunological and neurological senescence. PAM long bones (mainly consisting of cortical bone) display features of aging bone. Thus, we aimed to evaluate the vertebrae, representing a unique poorly loaded type of trabecular bone in mice, in PAM and no PAM (NPAM) controls. PAM showed an anxious behaviour, based on physical activity evaluation. These mice had decreased bone mineral density (0.078 mg/cm^2 in NPAM vs 0.070 g/cm^2 in PAM; $p<0.05$); a decreased number of osteocytes per bone field (404±36 in NPAM vs 320±27 in PAM; $p<0.01$); and downregulation of various osteoblastic genes and low eroded surface/bone surface, 4.2±0.5 in NPAM vs 1.9±0.2 in PAM; $p<0.01$). This was associated with increased expression of oxidative stress markers, Foxo1 and GADD45, in PAM vertebrae. Mesenchymal progenitors in the bone marrow of PAM have a poor mineralization capacity (assessed by the number of mineralized nodules and suface), and showed a lower response to an osteogenic input -represented by parathormone-related protein-, compared to NPAM. Collectively, these results indicate that PAM vertebrae show osteopenia related to diminished bone formation and remodeling. Our findings further support the validity of PAM as a suitable model for involutional osteoporosis and its treatment.

Key words: Premature aging, Osteoporosis, Oxidative stress.

Offprint requests to: Dr. Sergio Portal-Núñez, Laboratorio de Metabolismo Mineral y Óseo, Fundación Jiménez Díaz (Capio Group). Avda. Reyes Católicos, 2. 28040 Madrid, Spain. e-mail: sportal@fjd.es

Introduction

Osteoporosis is a major health concern in developed countries. The number of subjects suffering from this disease is increasing, with dramatic social and economic consequences to the health care systems (Reginster and Burlet, 2006). Aging together with estrogen depletion and an increased use of glucocorticoid-based medications have been related to this high osteoporosis prevalence (Kemink et al., 2000; Almeida et al., 2007b; Hofbauer et al., 2010).

Different approaches are envisioned to prevent the onset of osteopenia, including physical activity, which has been shown to improve bone quality both in rodents and humans (Umemura et al., 1997; Cullen et al., 2000; Heinonen et al., 2001; Wilks et al., 2009). This beneficial effect is a consequence of the so called "mechanosensing mechanisms" whereby bone can sense and translate mechanical stimuli into osteogenic responses (mechanotransduction) (Frost, 1987).

Aging might be explained as a imbalance between

the cellular levels of oxidants and antioxidants, according to the oxidation-inflammation hypothesis (Harman, 1956; De la Fuente and Miquel, 2009). Reactive oxygen species (ROS), namely superoxide ($O2^{\cdot-}$), hydroxyl radical ($OH^{\cdot-}$) and oxygen peroxide (H_2O_2), occur physiologically coupled to various intracellular signalling pathways (Janssen-Heininger et al., 2008). However, an excess of ROS production due to increased oxidative stress causes cellular damage leading to an impairment of cell physiology and eventually cell death (De la Fuente et al., 2005). Recent studies have demonstrated that ROS induce osteoblast apoptosis through an increased $p66^{Shc}$ phosphorylation (Almeida et al., 2007a; Jilka et al., 2010), and a decrease of osteoblast differentiation by hampering the osteogenic Wnt/ß-catenin pathway (Almeida et al., 2007a). The latter is accounted for by diversion of ß-catenin from TCF transcription elements to sequestration by forkhead box protein O (FoxO) transcription factors (Almeida et al., 2007a; Hoogeboom et al., 2008).

Premature aging mice (PAM) have been characterized as showing a poor response to stress related to neurological and immulogical features and increased ROS levels similar to those present in old mice and decreased life span (Guayerbas et al., 2002; Guayerbas and De La Fuente, 2003; De la Fuente, 2010; De la Fuente and Gimenez-Llort, 2010). It has been recently reported that PAM also exhibit phenotypic and genotypic characteristics of aging mice in their long bones (Portal-Núñez et al., 2013).

The present study was aimed to further assess the bone status of PAM. Since age-related osteopenia has been shown to occur early in mice and humans, mostly at the expense of a decline in trabecular structure (Glatt et al., 2007; Khosla et al., 2011), we focused on vertebral bone. In contrast to the long bones, vertebrae consist of mainly trabecular bone, and are not particularly prone to putative confounding effects of mechanical loading in mice.

Materials and methods

Mice

Adult female mice (24±2 week old) IRC/CD-1 were purchased from Harlan Ibérica (Barcelona, Spain). Mice were pathogen free, as tested by Harlan according to Federation of European Laboratory Science Associations' recommendations, and maintained (five animals/case) in a temperature-controlled room (22±2°C), with a 12-h light/dark reversed cycle. All mice were fed standard Sander Mus pellets (A04 diet, Panlab, Barcelona, Spain) and tap water *ad libitum*. Our protocol was approved by the Institutional Animal Care and Use Committees at the Instituto de Investigación Sanitaria (IIS)-Fundación Jiménez Díaz and UCM, following European Union guidelines and directives (86/6091 ECC).

Animals were sorted out as PAM or no PAM (NPAM) as previously described (Guayerbas et al., 2002; Guayerbas and De La Fuente, 2003). Briefly, mice at 29±2 weeks of age (4 weeks after arrival to the Animal Facility for quarantine and adaptation to the environment, according to Institutional well-being animal handling rules) were tested once a week for 4 consecutive weeks in a T-shaped maze. This apparatus essentially consists of three arms (10-cm wide, 25-cm long, and 10-cm high, each arm) made of wood covered in their internal face with black metacrylate. The floor is made of cylindrical aluminum rods (3-mm thick), placed perpendicularly to the side walls. To perform the test, the mouse was placed inside the vertical arm of the maze with its head facing the end wall. These tests were carried out between 9:00 and 11:00 h to minimize circadian variations, under red light. PAM were defined as those that complete the exploration in more than 10 seconds in all tests. Adult PAM (33±2 weeks old) and their NPAM counterparts, as well as NPAM at 15 months of age (aging mice controls) (n=8 per age/mouse type) were used.

PAM and NPAM mice were distributed in four cages (two animals per cage), respectively. The voluntary exercise was determined by a running wheel attached to the side wall of a standard cage and the distance (kilometers, Km), the time spent running (hours, h) and the average speed (Km/h) were measured daily for 7 days, using a magnetic sensor (Pareja-Galeano et al., 2012; Smythe and White, 2012).

After sacrifice by vertebral dislocation, mouse L1-L5 vertebrae were removed and cleaned of soft tissue, and snap-frozen and kept in liquid nitrogen until processing for histology (L1-L4) or total RNA extraction (L5). Immediately after sacrifice, bone marrow was flushed out from both tibiae and femora for cell culture, as previously described (Lozano et al., 2009; De Castro et al., 2012).

Bone densitometry

Bone mineral density (BMD) and bone mineral content (BMC) were determined in the dissected vertebrae (L1-L5) and tibiae by Dual-Energy X-ray absorptiometry using PIXImus (GE Lunar Corp., Madison, WI, USA). The PIXImus sotfware calculates the aforementioned parameters with a coefficient of variation 2%, and data are recorded in Microsoft Excell files (Microsoft Corp., Redmond, WA, USA) (Lozano et al., 2009)

Real time PCR

Total RNA was extracted from L5 samples with Trizol (Invitrogen, Groningen, The Netherlands). Synthesis of cDNA was performed using the high capacity cDNA reverse transcription kit following the manufacturer´s instructions (Applied Biosystems, Foster City, CA, USA). Real-time PCR was performed in an ABI PRISM 7500 system (Applied Biosystems) using

Premix ex Taq (Takara, Otsu, Japan) as described (Lozano et al., 2009). TaqMan MGB probes were obtained from Applied Biosystems (Assay-by-Design^{SM}) for gene amplification of FoxO1, growth arrest and DNA damage 45 (GADD45), osterix (OSX), osteoprotegerin (OPG), receptor activator of nuclear factor kappa-B ligand (RANKL) and runt-related transcription factor 2 (Runx2). The mRNA copy numbers were calculated for each sample using the cycle threshold (Ct) value, and normalized against 18S rRNA, as reported previously (Livak and Schmittgen, 2001; Lozano et al., 2009), and results were expressed as n-fold mRNA values vs corresponding levels in adult NPAM.

Bone histology and histomorphometry

The vertebral specimens (L1-L4) were dehydrated in graded ethanols and embedded in methylmethacrylate. Seven micron-thick sagittal longitudinal sections of the vertebrae were obtained with a rotation microtome for hard materials (Leica RM2255, Leica Microsystems, Nussloch, Germany), which were then stained with Goldner's trichrome. Histomorphometric measurements were performed using a light microscope with reticule-mounted eyepiece grid, and the following parameters were calculated according to the American Society for Bone and Mineral Research recommendations (Parfitt et al., 1987): bone volume per total tissue volume ratio (BV/TV), trabecular thickness (Tb.Th), trabecular separation (Tb.Sp), trabecular number (Tb.N), erosive surface per bone surface (ES/BS), osteoclast surface per bone surface (OcS/BS), number of osteoclasts per trabecular bone area (nOc/TA), osteoid volume/total tissue volume (OV/TV) and osteoid surface/bone surface (OS/BS) (Lozano et al., 2009; Nuche-Berenguer et al., 2011). The total number of osteoblasts per vertebra in each animal was also determined, and then the mean was calculated. The number of osteocytes were counted in four randomly selected bone areas per vertebrae at 200x magnification, calculating the mean per bone field. All histological evaluations were performed by at least two independet observers in a blinded fashion and the corresponding mean score ± standard error of mean (SEM) value was obtained for each mouse.

Bone marrow stromal cells (BMSCs) cultures

BMSCs were obtained from the intact tibiae and femora of PAM and NPAM at the time of sacrifice, as described previously (Lozano et al., 2009; De Castro et al., 2012). Briefly, the bone marrow was flushed out with α-Minimal Essential Medium containing 15% fetal bovine serum, 1% penicillin-streptomycin, and cell suspensions were prepared by aspirating the marrow through a 25-gauge needle. After centrifugation at 1500xg for 5 min, the cell pellets were resuspended in the same medium, and viable cells (by Trypan blue exclusion) were seeded at 1-2.5x10^6 cells per well onto six-well plates in 5% CO_2 at 37°C. Differentiation medium (the same medium with 50 μg/ml ascorbic acid and 10 mM ß-glycerophosphate) was added at day 3. Half of the volume of the cell-conditioned medium was exchanged every other day and, at the same time, PTHrP (1-36) was added at a final concentration of 100 nM to the corresponding wells. After 21 days, formed colonies were fixed with 75% ethanol, and matrix mineralization was determined by staining with 40 mM alizarin red S, quantifying the number of nodules, the total mineralized surface and the surface of mineralized nodules, using Photoshop cs 8.0.1 (Adobe Systems, San José, CA), as previously described (Lozano et al., 2009).

Statistics

Results are expressed as mean ± SEM throughout the text. Differences between experimental and control conditions were analyzed by using two-tail t-test or Mann-Whitney test, when appropriate. $p<0.05$ was considered significant. Statistical analysis was performed using statistical software (GraphPad InStat™ V2.04a).

Results

PAM vertebrae in contrast to long bones exhibit osteopenia

We first used DEXA to assess the status of bone in vertebrae (L1-L5) in NPAM and PAM (Table 1). PAM Vertebrae, which mainly consist of trabecular bone, display a reduction in BMD and BMC compared with corresponding NPAM. On the other hand, the tibiae from these mice -which were evaluated as control for changes in vertebrae in the same mice- showed a higher BMD than in those of their NPAM counterparts (Table 1). We hypothesised that the observed BMD differences might be due to the increased physical activity of PAM by their anxious behaviour. In fact, PAM showed more activity, based on evaluating running time and speed, and run distance, than their NPAM counterparts (Fig. 1).

Table 1. BMD and BMC in the tibia and vertebrae from PAM and NPAM.

Localization	Parameter	NPAM	PAM
Column (L1-L5)	BMD (g/cm2)	0.078±0.002	0.070±0.001*
	BMC (g)	0.040	0.035*
Tibia	BMD (g/cm2)	0.065±0.001	0.071±0.001*
	BMC (g)	0.023±0.001	0.026±0.001

BMD: Bone mineral density; BMC: Bone mineral content. Values represent mean±SEM (n=8); *p<0.05 vs NPAM.

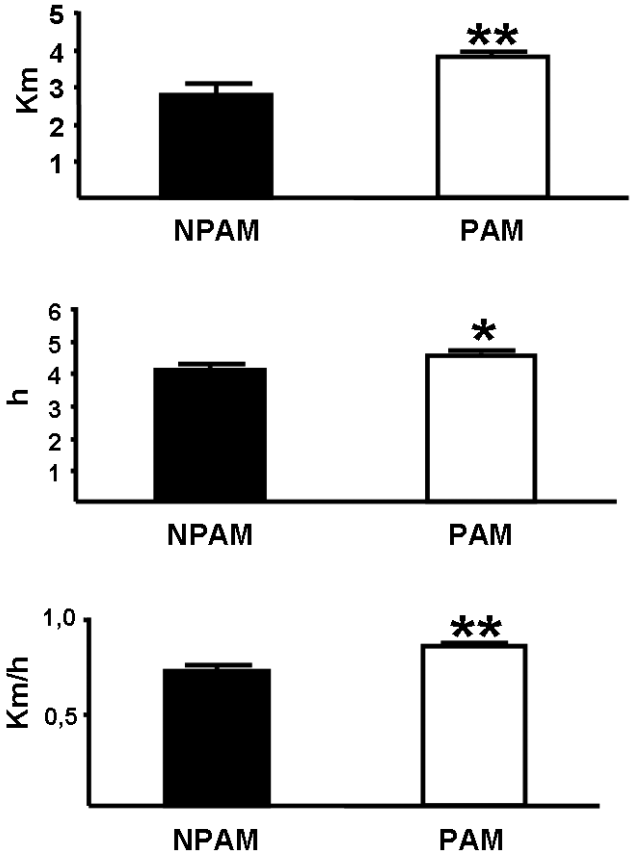

Fig. 1. PAM show more physical activity than NPAM. Graphics represent the distance (Km), time (hours) and speed (Km/h) developed by NPAM and PAM in a voluntary exercise in a running wheel attached to the side wall of a standard cage, measured using a magnetic sensor daily for 7 days. Mean ± SEM of data corresponding to 8 mice/group. *p<0.05 and **p<0.01 vs NPAM.

PAM vertebrae display low bone remodelling

We found a significant decrease in ES/BS as well as in OcS/BS and nOC/TA in L1-L4 of PAM vs NPAM (Table 2). On the other hand, a significant increase in the total number of osteoblasts occurred at this skeletal site in PAM. This increased abundance of osteoblasts was not accompanied by an augmented number of osteocytes, which was lower in PAM than in NPAM. Furthermore, less osteoid (newly formed non-

Table 2. Histomorphometric analysis of L1-L4 vertebrae in NPAM and PAM.

Parameter	NPAM	PAM
BV/TV (%)	24.8±1.5	27.1±1.6
TbTh (μm)	86.5±4.1	102.4±7.8
Tb Sp (μm)	271±22	275.5±13.8
Tb N (mm^{-1})	2.9±0.2	2.7±0.1
ES/BS (%)	4.2±0.5	1.9±0.2**
Ocs/BS (%)	1.3±0.2	0.7±0.1*
N.Oc/TA (mm^{-2})	0.5±0.1	0.2±0.1*
N Obs	8±2	17±2*
N Ost	404±36	320±27**
OV/TV (%)	0.3±0.09	0.06±0.04*
OS/BS (%)	2±0.8	0.3±0.13*

BV/TV (%): Bone volume/total tissue volume; TbTh: trabecular thickness; Tb Sp: trabecular separation; Tb N: trabecular Number; ES/BS: Erode surface/Bone surface; Ocs/BS: osteoclast/bone surface; N.Oc/TA: Osteoclast number/trabecular area; N.Obs: Total number of osteoblasts per vertebra; N.Ost: Number of osteocytes per field. OV/TV: Osteoid volume/total tissue volume; OS/BS: Osteoid surface/bone surface. Values represent mean±SEM (N=8/group). *p<0.05 and **p<0.01 vs NPAM.

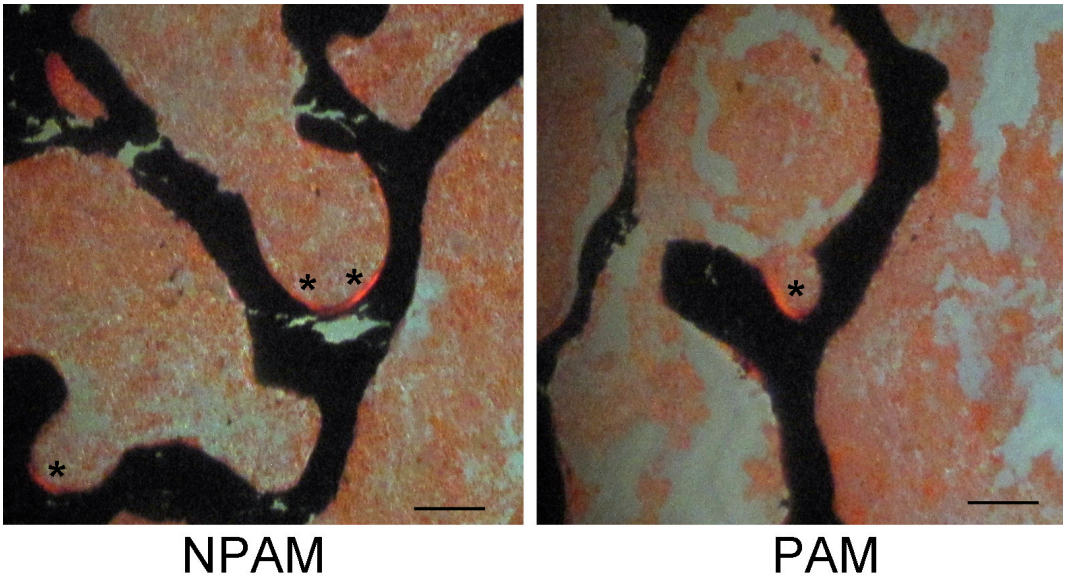

Fig. 2. Vertebrae show more osteoid surface in NPAM than in PAM. Stars (*) denote the birefringence of osteoid under polarized light. Representative images of a vertebrae from each group of mice (n=8). Scale bar: 100 μm.

mineralized bone matrix; OV/TV and OS/BS) was evident in PAM than in NPAM (Table 2, Fig. 2).

Changes in gene expression of bone-related factors in PAM vertebrae

The expression of FoxO1 and GADD45 was significantly increased in L5 vertebra of PAM compared with NPAM (Fig. 3A). Gene expression of Runx2 and Osterix, were downregulated at this skeletal site in PAM compared to NPAM (Fig. 3B). We found that the OPG/RANKL mRNA ratio was up-regulated in PAM-derived L5 (Fig. 3C, left panel), as a consequence of a decreased RANKL gene expression (Fig. 3C, right panel) without significant changes in that of OPG (not shown), compared to NPAM.

BMSCs from PAM display low osteogenic differentiation capacity

We found that the number of mineralization nodules as well as total and nodular mineralization surfaces were all significantly decreased in these cell cultures derived from adult PAM, and were similar to those in BMSCs from old NPAM (15 months of age) controls (Fig. 4A,B). It was shown that PTHrP (1-36), at 100 nM, was able to induce mineralization in these cell cultures from both types of mice tested, although it was of lower magnitude in those from both adult PAM and old NPAM than that observed in adult NPAM (Fig. 4A,B).

Discussion

In the present study, we show that adult PAM vertebrae exhibit osteopenia as assessed by low BMD and BMC, associated with alterations at both trabecular structure and bone remodeling factors. In contrast, and consistent with our previous report evaluating BMD in the whole animal (Portal-Núñez et al., 2013), the tibia from these mice showed an increased BMD. The mechanostat theory states that a bone homeostatic mechanism that responds to changes in mechanical loading governs bone remodeling (Frost, 1987). Exercise produces two opposite effects on bone: activation of bone remodeling, which might result in an increased bone density in both humans and rodents (Umemura et al., 1997; Cullen et al., 2000; Heinonen et al., 2001; Wilks et al., 2009), and an increase of microcracks leading to tissue fatigue. Therefore, in advanced involutional osteoporosis in which bone remodeling is compromised, exercise might increase the fracture risk

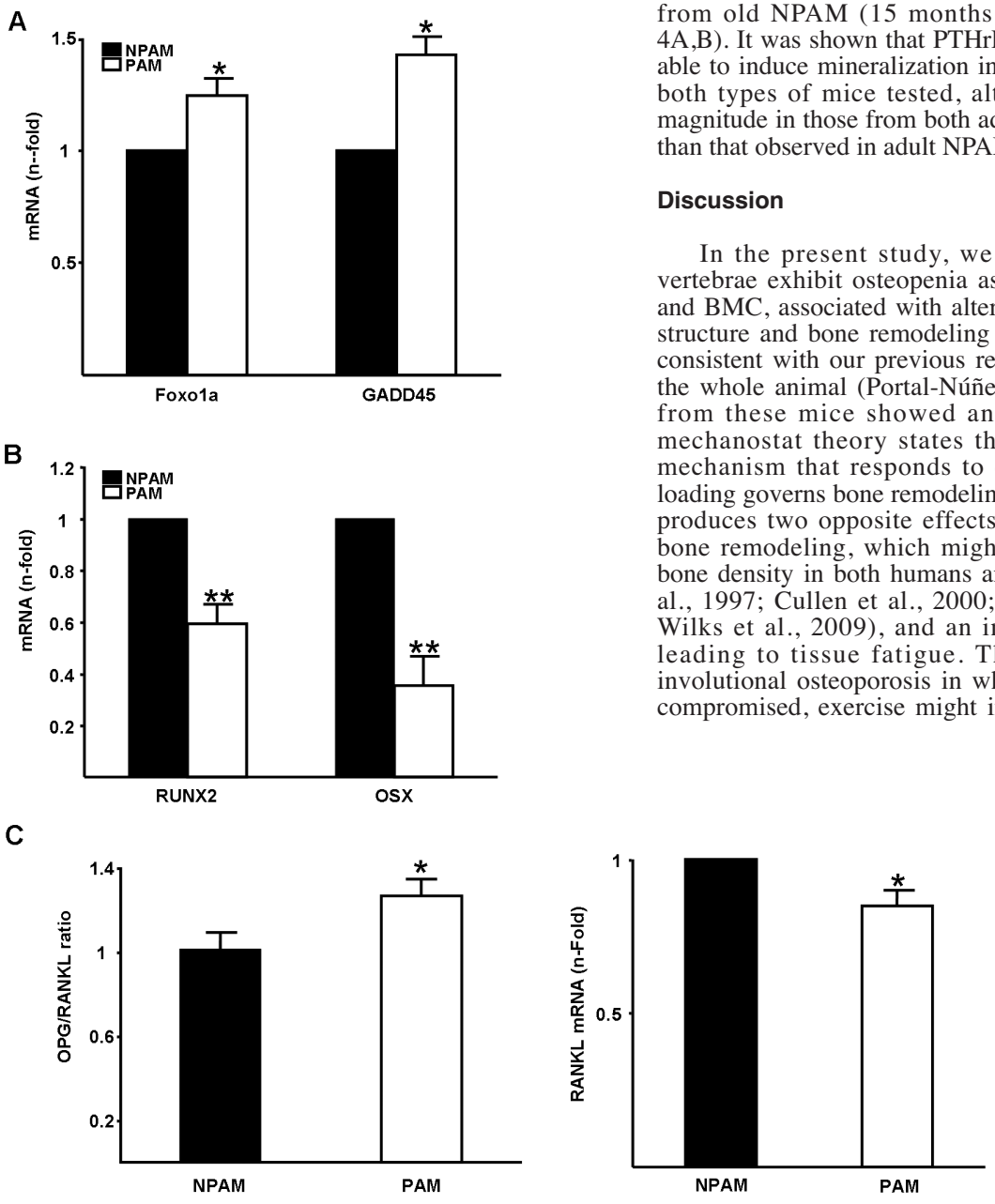

Fig. 3. Changes in the gene expression of different factors in vertebrae associated with the mouse type (NPAM or PAM). **A.** Gene expression of markers related to oxidative stress FoxO1 and GADD45. *p<0.05 vs NPAM (n=8). **B.** Gene expression of markers related to osteogenic status Runx2 and osterix. *p<0.05 vs NPAM (n=8). **C.** OPG/RANKL mRNA ratio and RANKL mRNA expression. *p<0.05 vs NPAM (n=8).

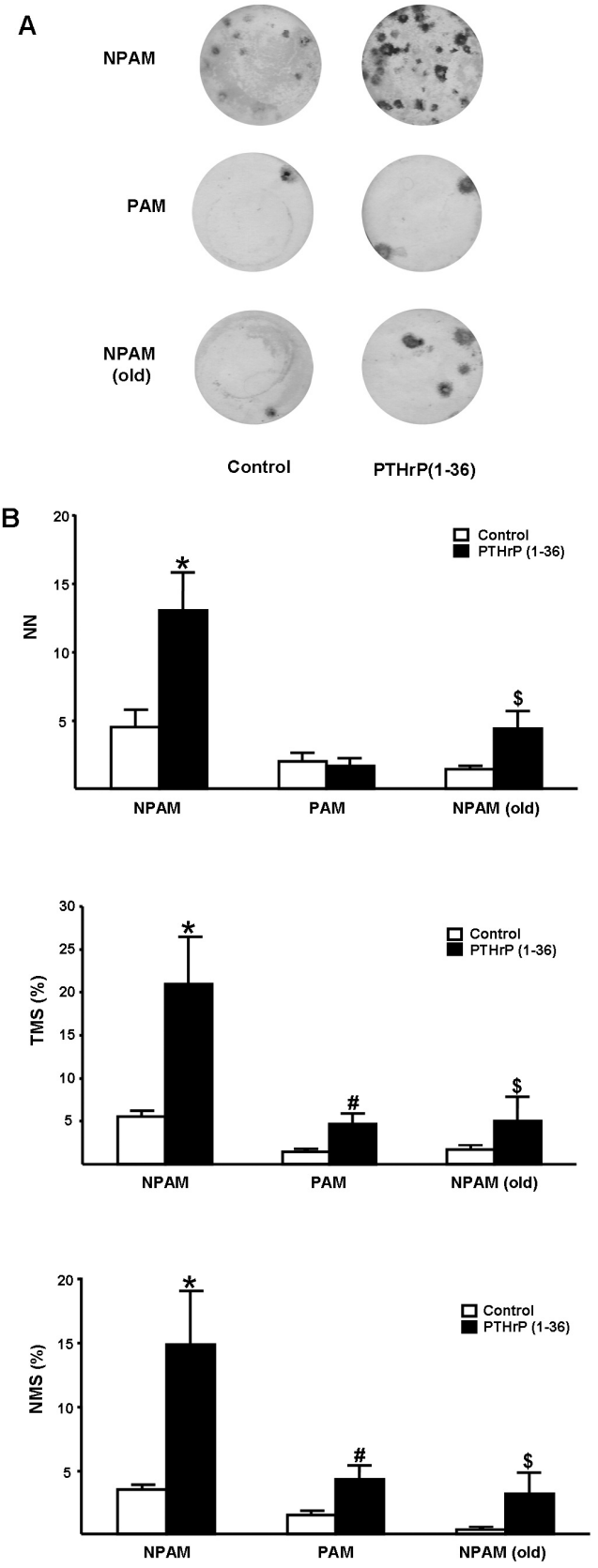

(Rittweger, 2006). Collectively, our recent findings (Portal-Núñez et al., 2013) and present data in adult PAM are consistent with the notion that increased physical activity caused by high anxiety in PAM (De la Fuente and Gimenez-Llort, 2010) might account for the increased bone mass and bone remodeling in load-bearing long bones.

We here analyzed the status of vertebra, a bone that is less prone to be affected by exercise than the long bones in rodents; thus, it might define more accurately the "basal" bone status of PAM. It was found that the lower bone mass in PAM vertebrae than that of their NPAM counterparts likely represents a reduction of bone remodeling. This fact is supported by the increased ratio of OPG/RANKL system which is a master paracrine regulator of osteoclastogenesis (Boyce and Xing, 2008; Kearns et al., 2008) and the apparent low resorption activity in PAM. Our findings also indicate that poorly differentiated osteoblasts, based on a reduced Runx2 and Osterix gene expression, both implicated in early osteoblast differentation (Franz-Odendaal et al., 2006), tend to accumulate in the vertebrae of these mice. In agreement with this contention, the number of osteocytes (terminally differentiated osteoblasts) and the amount of osteoid were significantly decreased in adult PAM vertebrae as compared to those in NPAM controls. These aggregated data indicate an altered osteoblast differentiation and function, suggesting the existence of a low bone remodeling status in PAM vertebrae. However, the reason for this osteoblast differentiation impairment is presently unknown. PAM also display increased levels of glucocorticoids (Pérez-Alvárez et al., 2005), which might contribute to the development of osteopenia through favoring osteocyte and osteoblast apoptosis (Weinstein et al., 1998, 2000). Alternately, the apparent deficit of osteoblast differentiation in PAM might be related to the inhibition of Wnt/ß-catenin pathway a key factor in osteoblast differentiation (Glass et al., 2005) produced by the increased oxidative stress in PAM (Almeida et al., 2007a; Hoogeboom et al., 2008). In this regard, in our recent report (Portal-Núñez et al., 2013), we found that ß-catenin protein was significantly decreased in the PAM tibia.

Oxidative stress appears to have a major pathogenic role in bone loss development (Manolagas, 2010). In this respect, an increase in oxidative stress status has been reported to occur in the immune system (Guayerbas and

Fig. 4. PTHrP (1-36) can compensate for the lack of differentiation in BMSCs from PAM. BMSC cultures from adult NPAM, PAM and old NPAM, treated or not with PTHrP (1-36) (100 nM) every other day, at day 21. **A.** Representative images of alizarin red S staining are shown. **B.** Changes in the number of mineralized nodules (NN), total mineralized suface (TMS) and nodular mineralized surface (NMS) in the different mouse groups studied. Mean ± SEM (n=6 wells/group); *p<0.05 vs NPAM control; #p<0.05 vs PAM control, $p<0.05 vs NPAM (old) control.

De La Fuente, 2003; De la Fuente, 2010) as well as in other organs, such as brain of PAM (Viveros et al., 2007; De la Fuente and Miquel, 2009). Moreover, we recently showed elevated expression of both oxidative stress-related genes FoxO1 and catalase (Almeida et al., 2007b; Ambrogini et al., 2010) and the pro-inflammatory chemokine MCP-1 in PAM long bones (Portal-Núñez et al., 2013). Consistently, we found here an increased oxidative stress, as denoted by a high FoxO1 and GADD45 overexpression, in PAM vertebrae. Of note, it has been recently reported that KO mice for superoxide dismutase 1 (an important mechanist of defense anti oxidative stress) present a low bone remodeling state (Nojiri et al., 2011). It has been shown that oxidative stress decreases the differentiation capacity and the number of osteoblast progenitors in the bone marrow (Jilka et al., 1998; Manolagas, 2010; Almeida, 2011). In the present study, we show that BMSCs isolated from PAM exhibited less mineralization capacity than those from NPAM when grown in an osteogenic medium.

Several studies have shown that inhibition of oxidative stress by using common anti-oxidants can prevent its deleterious effects in various tissues and organs (Hughes, 1999; Kaneto et al., 1999; Lin et al., 2008). However, in bone, most of these agents inhibit osteoclastogenesis and the osteogenic Wnt-pathway (Funato et al., 2006), and thus impair bone remodeling (Lean et al., 2003; Almeida et al., 2007a). In contrast, PTH stimulates these pathways and also exhibits anti-oxidative stress features to induce bone accrual (Almeida et al., 2007a,b; Jilka et al., 2010). In an attempt to examine the osteogenic capacity of a well characterized bone anabolic agent, namely PTHrP (1-36) that also inhibits oxidative stress (Lozano et al., 2009; De Castro et al., 2012; Esbrit and Alcaraz, 2013), in aging bone, we exposed PAM and NPAM-derived BMSCs to this peptide in an osteoblastic differentiation medium. Our findings demonstrate that exposure to this peptide can increase the mineralization capacity of these cells from both PAM and NPAM groups.

Our aggregated findings in the PAM model strongly suggest the existence of a low turnover status in vertebrae, a trabecular bone type poorly exposed to mechanical stimuli in rodents. This is a different scenario than that in humans, whose spine is prone to bear mechanical loading. Although it should be emphasized that trabecular bone loss already starts in younger men and women, before a decrease of sex steroid levels in the latter (Khosla et al., 2011).

In summary, we here demonstrate that PAM show an anxious behaviour which might confer a certain protection in their long bones but not in vertebrae. In the latter bone type, PAM display a decrease in bone mass, an impairment of osteoblast differentiation related to a decreased bone remodeling, and their mesenchymal progenitors exhibit a low mineralization capacity. Taken together, our data confirm PAM as an advantageous model for studies on the pathogenesis of involutional osteoporosis and its treatment.

Acknowledgements. We thank A.F. Stewart, M.D. and A. García-Ocaña, Ph.D. (Department of Endocrinology and Metabolism, University of Pittsburgh School of Medicine, Pittsburgh, PA) for generously providing PTHrP (1-36). This work was supported by grants from Instituto de Salud Carlos III (PI11/00449, RD06/0013/1002, RD12/0043/0008 and RD12/0043/0018) and Fundación Española para la Investigación Ósea y Metabolismo Mineral (FEIOMM). S.P.-N. and J.C. are recipients of a post-doctoral research contract from RETICEF (RD06/0013/1002, RD12/0043/0008 and RD06/0013/0003, RD12/0043/0018). D.L. and J.A.A. are the recipients of a post-doctoral research contract from Comunidad Autónoma de Madrid (S-2009/MAT-1472) and the Spanish Ministerio de Ciencia e Innovación (MICINN)-Juan de la Cierva program (JCI-2009-04360), respectively.

References

Almeida M. (2011). Unraveling the role of foxos in bone--insights from mouse models. Bone 49, 319-327.

Almeida M., Han L., Martin-Millan M., O'Brien C.A. and Manolagas S.C. (2007a). Oxidative stress antagonizes wnt signaling in osteoblast precursors by diverting beta-catenin from t cell factor- to forkhead box o-mediated transcription. J. Biol. Chem. 282, 27298-27305.

Almeida M., Han L., Martin-Millan M., Plotkin L.I., Stewart S.A., Roberson P.K., Kousteni S., O'Brien C.A., Bellido T., Parfitt A.M., Weinstein R.S., Jilka R.L. and Manolagas S.C. (2007b). Skeletal involution by age-associated oxidative stress and its acceleration by loss of sex steroids. J. Biol. Chem. 282, 27285-27297.

Ambrogini E., Almeida M., Martin-Millan M., Paik J.H., Depinho R.A., Han L., Goellner J., Weinstein R.S., Jilka R.L., O'Brien C.A. and Manolagas S.C. (2010). Foxo-mediated defense against oxidative stress in osteoblasts is indispensable for skeletal homeostasis in mice. Cell. Metab. 11, 136-146.

Boyce B.F. and Xing L. (2008). Functions of rankl/rank/opg in bone modeling and remodeling. Arch. Biochem. Biophys. 473, 139-146.

Cullen D.M., Smith R.T. and Akhter M.P. (2000). Time course for bone formation with long-term external mechanical loading. J. Appl. Physiol. 88, 1943-1948.

De Castro L.F., Lozano D., Portal-Núñez S., Maycas M., De la Fuente M., Caeiro J.R. and Esbrit P. (2012). Comparison of the skeletal effects induced by daily administration of pthrp (1-36) and pthrp (107-139) to ovariectomized mice. J. Cell. Physiol. 227, 1752-1760.

De la Fuente M. (2010). Murine models of premature ageing for the study of diet-induced immune changes: Improvement of leucocyte functions in two strains of old prematurely ageing mice by dietary supplementation with sulphur-containing antioxidants. Proc. Nutr. Soc. 69, 651-659.

De la Fuente M. and Miquel J. (2009). An update of the oxidation-inflammation theory of aging: The involvement of the immune system in oxi-inflamm-aging. Curr. Pharm. Des. 15, 3003-3026.

De la Fuente M. and Gimenez-Llort L. (2010). Models of aging of neuroimmunomodulation: Strategies for its improvement. Neuroimmunomodulation 17, 213-216.

De la Fuente M., Hernanz A. and Vallejo M.C. (2005). The immune system in the oxidative stress conditions of aging and hypertension: Favorable effects of antioxidants and physical exercise. Antioxid. Redox. Signal 7, 1356-1366.

Esbrit P. and Alcaraz M.J. (2013). Current perspectives on parathyroid

hormone (PTH) and PTH-related protein (PTHrP) as bone anabolic therapies. Biochem. Pharmacol. 85, 1417-1423.

Franz-Odendaal T.A., Hall B.K. and Witten P.E. (2006). Buried alive: How osteoblasts become osteocytes. Dev. Dyn. 235, 176-190.

Frost H.M. (1987). Bone "mass" and the "mechanostat": A proposal. Anat. Rec. 219, 1-9.

Funato Y., Michiue T., Asashima M. and Miki H. (2006). The thioredoxin-related redox-regulating protein nucleoredoxin inhibits wnt-beta-catenin signalling through dishevelled. Nat. Cell. Biol. 8, 501-508.

Glass D.A., Bialek P., Ahn J.D., Starbuck M., Patel M.S., Clevers H., Taketo M.M., Long F., McMahon A.P., Lang R.A. and Karsenty G. (2005). Canonical wnt signaling in differentiated osteoblasts controls osteoclast differentiation. Dev. Cell 8, 751-764.

Glatt V., Canalis E., Stadmeyer L. and Bouxsein M.L. (2007). Age-related changes in trabecular architecture differ in female and male c57bl/6j mice. J. Bone. Miner. Res. 22, 1197-1207.

Guayerbas N. and De La Fuente M. (2003). An impairment of phagocytic function is linked to a shorter life span in two strains of prematurely aging mice. Dev. Comp. Immunol. 27, 339-350.

Guayerbas N., Puerto M., Victor V.M., Miquel J. and De la Fuente M. (2002). Leukocyte function and life span in a murine model of premature immunosenescence. Exp. Gerontol. 37, 249-256.

Harman D. (1956). Aging: A theory based on free radical and radiation chemistry. J. Gerontol. 11, 298-300.

Heinonen A., Sievanen H., Kyrolainen H., Perttunen J. and Kannus P. (2001). Mineral mass, size, and estimated mechanical strength of triple jumpers' lower limb. Bone 29, 279-285.

Hofbauer L.C., Hamann C. and Ebeling P.R. (2010). Approach to the patient with secondary osteoporosis. Eur. J. Endocrinol. 162, 1009-1020.

Hoogeboom D., Essers M.A., Polderman P.E., Voets E., Smits L.M. and Burgering B.M. (2008). Interaction of foxo with beta-catenin inhibits beta-catenin/t cell factor activity. J. Biol. Chem. 283, 9224-9230.

Hughes D.A. (1999). Effects of dietary antioxidants on the immune function of middle-aged adults. Proc. Nutr. Soc. 58, 79-84.

Janssen-Heininger Y.M., Mossman B.T., Heintz N.H., Forman H.J., Kalyanaraman B., Finkel T., Stamler J.S., Rhee S.G. and van der Vliet A. (2008). Redox-based regulation of signal transduction: Principles, pitfalls, and promises. Free Radic. Biol. Med. 45, 1-17.

Jilka R.L., Takahashi K., Munshi M., Williams D.C., Roberson P.K. and Manolagas S.C. (1998). Loss of estrogen upregulates osteoblastogenesis in the murine bone marrow. Evidence for autonomy from factors released during bone resorption. J. Clin. Invest. 101, 1942-1950.

Jilka R.L., Almeida M., Ambrogini E., Han L., Roberson P.K., Weinstein R.S. and Manolagas S.C. (2010). Decreased oxidative stress and greater bone anabolism in the aged, when compared to the young, murine skeleton with parathyroid hormone administration. Aging Cell 9, 851-867.

Kaneto H., Kajimoto Y., Miyagawa J., Matsuoka T., Fujitani Y., Umayahara Y., Hanafusa T., Matsuzawa Y., Yamasaki Y. and Hori M. (1999). Beneficial effects of antioxidants in diabetes: Possible protection of pancreatic beta-cells against glucose toxicity. Diabetes 48, 2398-2406.

Kearns A.E., Khosla S. and Kostenuik P.J. (2008). Receptor activator of nuclear factor kappab ligand and osteoprotegerin regulation of bone remodeling in health and disease. Endocr. Rev. 29, 155-192.

Kemink S.A., Hermus A.R., Swinkels L.M., Lutterman J.A. and Smals A.G. (2000). Osteopenia in insulin-dependent diabetes mellitus; prevalence and aspects of pathophysiology. J. Endocrinol. Invest. 23, 295-303.

Khosla S., Melton L.J. 3rd and Riggs B.L. (2011). The unitary model for estrogen deficiency and the pathogenesis of osteoporosis: Is a revision needed? J. Bone Miner. Res. 26, 441-451.

Lean J.M., Davies J.T., Fuller K., Jagger C.J., Kirstein B., Partington G.A., Urry Z.L. and Chambers T.J. (2003). A crucial role for thiol antioxidants in estrogen-deficiency bone loss. J. Clin. Invest. 112, 915-923.

Lin C.L., Wang J.Y., Ko J.Y., Surendran K., Huang Y.T., Kuo Y.H. and Wang F.S. (2008). Superoxide destabilization of beta-catenin augments apoptosis of high-glucose-stressed mesangial cells. Endocrinology 149, 2934-2942.

Livak K.J. and Schmittgen T.D. (2001). Analysis of relative gene expression data using real-time quantitative pcr and the 2(-delta delta c(t)) method. Methods 25, 402-408.

Lozano D., de Castro L.F., Dapia S., Andrade-Zapata I., Manzarbeitia F., Alvárez-Arroyo M.V., Gómez-Barrena E. and Esbrit P. (2009). Role of parathyroid hormone-related protein in the decreased osteoblast function in diabetes-related osteopenia. Endocrinology. 150, 2027-2035.

Manolagas S.C. (2010). From estrogen-centric to aging and oxidative stress: A revised perspective of the pathogenesis of osteoporosis. Endocr. Rev. 31, 266-300.

Nojiri H., Saita Y., Morikawa D., Kobayashi K., Tsuda C., Miyazaki T., Saito M., Marumo K., Yonezawa I., Kaneko K., Shirasawa T. and Shimizu T. (2011). Cytoplasmic superoxide causes bone fragility owing to low-turnover osteoporosis and impaired collagen cross-linking. J. Bone Miner. Res. 26, 2682-2694.

Nuche-Berenguer B., Lozano D., Gutierrez-Rojas I., Moreno P., Marinoso M.L., Esbrit P. and Villanueva-Penacarrillo M.L. (2011). Glp-1 and exendin-4 can reverse hyperlipidic-related osteopenia. J. Endocrinol. 209, 203-210.

Pareja-Galeano H., Brioche T., Sanchis-Gomar F., Escriva C., Dromant M., Gomez-Cabrera M.C. and Vina J. (2012). Effects of physical exercise on cognitive alterations and oxidative stress in an app/psn1 transgenic model of alzheimer's disease. Rev. Esp. Geriatr. Gerontol. 47, 198-204. (in spanish).

Parfitt A.M., Drezner M.K., Glorieux F.H., Kanis J.A., Malluche H., Meunier P.J., Ott S.M. and Recker R.R. (1987). Bone histomorphometry: Standardization of nomenclature, symbols, and units. Report of the asbmr histomorphometry nomenclature committee. J. Bone Miner. Res. 2, 595-610.

Pérez-Alvarez L., Baeza I., Arranz L., Marco E.M., Borcel E., Guaza C., Viveros M.P. and De la Fuente M. (2005). Behavioral, endocrine and immunological characteristics of a murine model of premature aging. Dev. Comp. Immunol. 29, 965-976.

Portal-Núñez S., Manassra R., Lozano D., Acitores A., Mulero F., Villanueva-Penacarrillo M.L., De la Fuente M. and Esbrit P. (2013). Characterization of skeletal alterations in a model of prematurely aging mice. Age (Dordr). 35, 383-393.

Reginster J.Y. and Burlet N. (2006). Osteoporosis: A still increasing prevalence. Bone 38, S4-9.

Rittweger J. (2006). Can exercise prevent osteoporosis? J. Musculoskelet. Neuronal. Interact. 6, 162-166.

Smythe G.M. and White J.D. (2012). Voluntary wheel running in

dystrophin-deficient (mdx) mice: Relationships between exercise parameters and exacerbation of the dystrophic phenotype. PLoS Curr. 3, RRN1295.

Umemura Y., Ishiko T., Yamauchi T., Kurono M. and Mashiko S. (1997). Five jumps per day increase bone mass and breaking force in rats. J. Bone Miner. Res. 12, 1480-1485.

Viveros M.P., Arranz L., Hernanz A., Miquel J. and De la Fuente M. (2007). A model of premature aging in mice based on altered stress-related behavioral response and immunosenescence. Neuroimmunomodulation 14, 157-162.

Weinstein R.S., Jilka R.L., Parfitt A.M. and Manolagas S.C. (1998). Inhibition of osteoblastogenesis and promotion of apoptosis of osteoblasts and osteocytes by glucocorticoids. Potential mechanisms of their deleterious effects on bone. J. Clin. Invest. 102, 274-282.

Weinstein R.S., Nicholas R.W. and Manolagas S.C. (2000). Apoptosis of osteocytes in glucocorticoid-induced osteonecrosis of the hip. J. Clin. Endocrinol. Metab. 85, 2907-2912.

Wilks D.C., Winwood K., Gilliver S.F., Kwiet A., Chatfield M., Michaelis I., Sun L.W., Ferretti J.L., Sargeant A.J., Felsenberg D. and Rittweger J. (2009). Bone mass and geometry of the tibia and the radius of master sprinters, middle and long distance runners, race-walkers and sedentary control participants: A pqct study. Bone 45, 91-97.

Accepted May 13, 2013